Effect of Nickel-containing Ligand on Thermal Stability and Combustible Property of Poly(lactic acid)

XUEYING SHAN [1,2,3], SIUMING LO [2**], QILONG TAI [1,2,3], ZHOU GUI[1],YUAN HU [1,3*] and SAIHUA JIANG [1,2,3]
[1]State Key Laboratory of Fire Science, University of Science and Technology of China, and USTC-CityU Joint Advanced Research Centre, Suzhou, China
[2]Department of Civil and Architectural Engineering, City University of Hong Kong, and USTC-CityU Joint Advanced Research Centre, Suzhou, China
[3]Suzhou Key Laboratory of Urban Public Safety, Suzhou Institute of University of Science and Technology of China, Suzhou, China

ABSTRACT

Nickel-containing ligand (L.) decorated with molybdenum and 1h-pyrazole template was prepared by the hydrothermal method. Then it was added in poly(lactic acid) (PLA) matrix. One goal of this work was to investigate the effect of L. on thermal stability and combustible property of PLA matrix. The structure and property of L. were characterized by fourier transform infrared (FTIR), X-ray photoelectron spectroscopy (XPS) and thermogravimetric analysis (TGA). The thermal properties of composites were tested by TGA, differential scanning calorimetry (DSC) and real time fourier transform infrared (RTIR). Combustible properties were researched by microscale combustion calorimetry (MCC). The volatilized products after the sample pyrolysis were also discussed. The thermal stability and combustible property analyses indicated that L. had positive effect in PLA matrix. Dynamic mechanical analysis (DMA) was used to measure the mechanical strength of PLA composites.

KEYWORDS: composite; thermal property; heat release rate; catalyst.

INTRODUCTION

Packaging is the main market for plastic material consumption, which includes flexible films and rigid containers. It has a problem for post-consumption disposal of wastes. Biodegradable polymers as alternatives to plastic materials are widely used in packaging industry [1,2]. In particular, poly(lactic acid) (PLA) has received an increasing amount of attention because its raw material, lactic acid, can be efficiently produced by fermentation from renewable resources [3,4]. Moreover, it has good properties such as thermoplastic, a large melting point, a high degree of transparency and ease of fabrication [5]. Unfortunately, owing to its intrinsic chemical composition and molecular structure, there are still some disadvantages that limit its further application and development, such as low thermal stability, low mechanical property and high flammability [6,7]. Therefore, the improvement of these properties is still a very important target in academic research and industrial applications.

To resolve the above problems, inorganic additives have been reported [8-11]. Among these investigations, it is noted that additives could improve the thermal stability and flame retardancy of PLA whereas its mechanical properties are decreased because of poor interfacial compatibility between the filler and polymer. In fact, many efforts have been made to improve the mechanical properties of PLA in recent years. The addition of cellulose nanocrystal is the most common method to reinforce PLA [12-14]. However, it cannot reduce the fire risk of PLA.

Nickel-containing ligands could form interesting structure with potential applications in the areas of catalysis, ion exchange, molecular sieves, magnetism and intercalation chemistry [15-17]. In our present work, we synthesized nickel-containing ligand (L.) decorated with molybdenum using the hydrothermal synthesis technique and 1h-pyrazole template. Then L. was added in PLA matrix. The effect of L. on the thermal stability, combustible property and mechanical property of PLA matrix was investigated.

∗∗ Corresponding Author. Tel.: (852) 34427683.
E-mail: bcsmli@cityu.edu.hk

∗ Corresponding Author. Tel./fax: +86-551-63601664.
E-mail: yuanhu@ustc.edu.cn

EXPERIMENTAL SECTION

Materials and Measurements

PLA (model 2002D) was supplied by Polymer UNIC Technology Co., Ltd (Suzhou, China). 1H-pyrazole was bought from Sa En Chemical Technology Co., Ltd (Shanghai, China). Nickel (II) chloride hexahydrate, sodium molybdate dihydrate, orthophosphoric acid and ethanol were purchased from Sinopharm Chemical Reagent Co., Ltd. (Shanghai, China).

Fourier transform infrared (FTIR) spectra were obtained on a Nicolet 6700 FT-IR spectrophotometer. X-ray photoelectron spectroscopy (XPS) was conducted with an ESCALAB 250 electron spectrometer (Thermo-VG Scientific Co.). Thermogravimetric analysis (TGA) was conducted from 100 to 700˚C using a Q5000IR thermoanalyzer instrument under a flowing air atmosphere at a scan rate of 10˚C/min. Differential scanning calorimetry (DSC) measurements were performed using a NETZSCH DSC (204 F1 Phoenix) at a heating rate of 10˚C/min in a nitrogen atmosphere. The first scan was designed to erase the thermal history of the samples. The data reported was collected from the second scan. Real time fourier transform infrared (RTIR) spectra were recorded using a MAGNA-IR 750 spectrophotometer (Nicolet Instrument Company, USA) equipped with a ventilated oven having a heating device. The temperature of the oven was raised at a heating rate of 10˚C/min. Dynamic FTIR spectra were obtained in situ during thermal oxidative degradation of PLA composites. MCC tests were used to investigate the combustion behavior of all samples according to ASTM D 7309-07. 4-8 mg of each sample was heated at 1˚C/s and held there for 30 seconds. During pyrolysis, the volatilized decomposition products were transferred in the stream of nitrogen to a high-temperature combustion furnace where pure oxygen was added and the decomposition products were completely combusted. The amount of oxygen consumed was measured with an oxygen analyzer and used to calculate a heat release rate (HRR). Thermogravimetric analysis/infrared spectrometry (TGA-IR) was performed to analyze the volatilized products after the sample pyrolysis under the nitrogen flow of 35.0 ml/min at a heating rate of 20˚C/min. Dynamic mechanical analysis (DMA) was conducted with the Perkin Elmer Pyris Diamond from 30 to 120˚C at a heating rate of 5˚C/min with a frequency of 10 Hz in the tensile configuration.

Preparaion of L. and PLA Composites

L. was synthesized by the hydrothermal method and the synthetic route was described in Fig. 1 (a). $NiCl_2 \cdot 6H_2O$, pz and $Na_2MoO_4 \cdot 2H_2O$ (the molar ratio was 1:6:3) were dissolved in distilled water by vigorous stirring, accordingly a stable colloid was obtained. The pH value was adjusted to 7 using 1 mol/L H_3PO_4. The resulting mixture was stirred vigorously for 30 min to ensure the proper mixing of the components, and then sealed in a Teflon-lined stainless-steel autoclave. The autoclave temperature was raised up to 120˚C slowly and kept for 2 days. The autoclave was cooled to room temperature when the reaction was completed. Then the solid product was collected by filtration and washed by deionized water and anhydrous ethanol, respectively. After dried in a vacuum oven at 60˚C, L. was characterized by FTIR, XPS and TGA.

PLA composites were melted and mixed in a twin-roller mixer at a rotor speed of 40 rpm and at a temperature of 175˚C for 10 min. PLA was dried in an oven at 70˚C for 12 h before use. PLA1, PLA2, PLA3, PLA4 and PLA5 composites contained 0, 1 wt%, 3 wt%, 5 wt% and 8 wt% L., respectively.

RESULTS AND DISCUSSION

FTIR, XPS and TGA Characterizations of L.

The cluster anion $[P_2Mo_5]$ consists of edge and corner, which shares MoO_6 octahedra and forms Mo_5O_{15} ring capped by two PO_4 tetrahedrons. Each phosphate subunit shares three oxo-group with the molybdate ring. Ni units link $[P_2Mo_5]$ clusters to form 2D sheets and connect the sheets to produce a double sheet. The free pz moieties are linked to $[P_2Mo_5]$ clusters. H-bond interactions are mediated by $[Ni(pz)_4(H_2O)_2]$ units [17,18]. The FTIR spectrum of L. is present in Fig. 1(b). The peak at 3396 cm^{-1} is attributed to O-H stretching vibration. The absorption at 2355 cm^{-1} and 1634 cm^{-1} is assigned to C-H. The peak at 1530 cm^{-1} corresponds to C=C stretching vibration. The peaks at 1200~800 cm^{-1} are attributed to P-O tetrahedron characteristic peaks [19] and 951~735 cm^{-1} peaks indicate the stretching vibration of Mo-O, Mo-O-Ni and Mo-O-P [20]. They have partial overlap. Therefore, the absorption peaks in 951~800 cm^{-1} region are

strong. The peak at 452 cm^{-1} is assigned to Ni-N. The above analyses demonstrate that L. is synthesized successfully.

The spectrum of element analyses (XPS) is shown in Fig. 1(c). The peaks at approximately 133.1, 232.3, 284.8, 400.5, 530.5 and 856.0 eV are attributed to P_{2p}, Mo_{3d}, C_{1s}, N_{1s}, O_{1s} and Ni_{2p}, respectively. The corresponding weight percentages are P 1.41%, Mo 5.82%, C 39.16%, N 14.25%, O 31.15% and Ni 8.22%. The calculated result suggests the formula $(pz)_{11.19}Ni_{3.08}PMo_{1.33}O_{42.79}\cdot(H_2O)_n$.

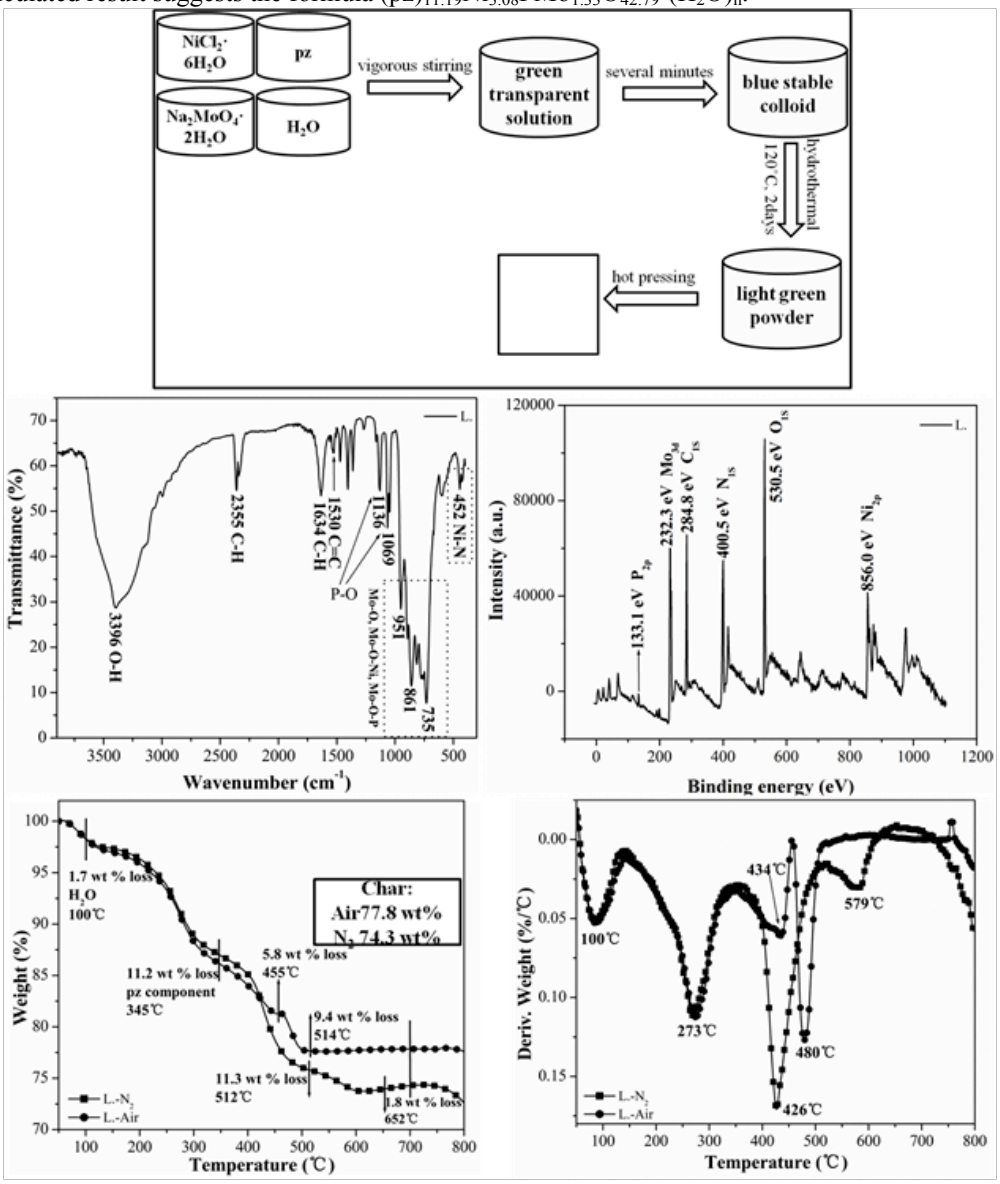

Fig. 1. (a) The synthetic route of L.; (b) The IR spectrum of L.; (c) The XPS spectrum of L.; (d) TGA curves of L. in N_2 and air atmosphere; (e) DTG curves of L. in N_2 and air atmosphere.

TGA and the corresponding differential thermogravimetry (DTG) curves of L. in N_2 and air atmosphere are shown in Fig. 1(d) and Fig. 1(e), respectively. The 1.7 wt% water molecules are lost below 100˚C. The weight loss is 11.2 wt% in 100~345˚C corresponding to the partial release of pz molecules. The curve of N_2 atmosphere is different from air in the range of 345~800˚C. The weight loss for N_2 curve is 11.3 wt% from 345 to 512˚C, owing to the further degradation of pz and destruction of phosphomolybdate framework [18]. The structure of L. is destroyed above 512˚C. There is 1.8 wt% loss in the temperature rang 512~652˚C. The loss is 5.8 wt% and 9.4 wt% for air curve in the range of 345~455˚C and 455~514˚C, respectively. The char residue of L. at 700˚C in air atmosphere is 77.8 wt%, which is higher than that of in N_2 (74.3 wt%). It is due to TGA measures the thermal decomposition of L. under air atmosphere, and there is oxygen

participation. The peaks of DTG curves are presented by Fig. 1 (e), corresponding to the highest degradation or decomposition rate of each stage.

Thermal Properties of PLA Composites

Figure 2(a) describes the DSC thermograms of PLA composites. The specific thermal property of PLA matrix is altered after adding L.. The glass transition temperature (T_g) is shifted to a low temperature region. It is changed from 60.2˚C for PLA1 to 51.4˚C for PLA5, and decreased when L. content is increased. It might be attributed to the presence of the phase interface between PLA and L., which results in enhancing chain mobility near interface [21]. Thus, the plasticity of PLA is improved. The thermal decomposition behaviors of PLA composites are investigated by TGA. The 2 wt% loss temperature ($T_{-2\ wt\%}$), the maximum mass loss temperature (T_{max}) and the char residue at 700˚C are listed in Table 1. Figure. 2 (b) shows the TGA curves of PLA composites in air atmosphere. The decomposition of virgin PLA occurs by a two-step process. It can be seen from Table 1 that the decomposition behaviors are changed apparently. The value of $T_{-2\ wt\%}$ and T_{max} is shifted to a low temperature region with the addition of L., and it is decreased with the amount of L. increase. It might be due to the transition metal elements catalysis or the partial release of pz molecules. The char residue of PLA composites is improved from 0.6 wt% for PLA1 to 4.9 wt% for PLA5.

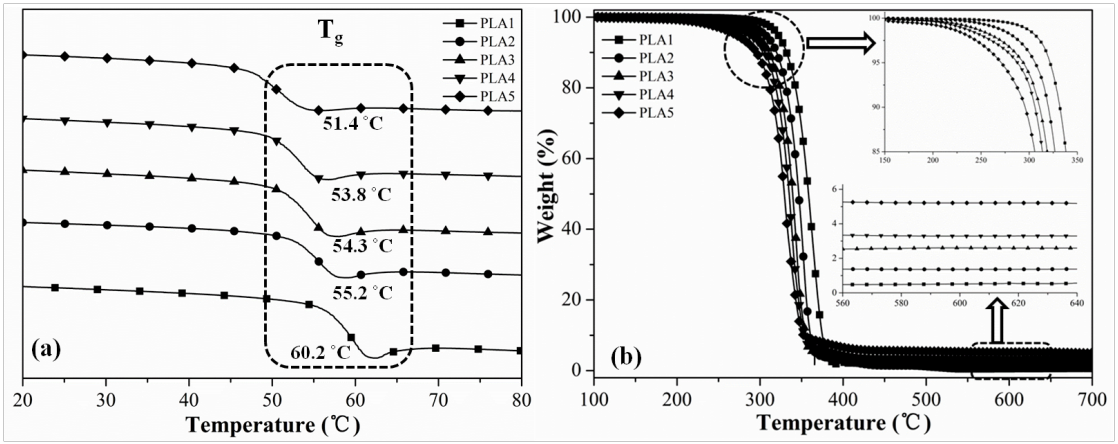

Fig. 2. (a) DSC curves of PLA composites; (b) TGA curves of PLA composites.

Table 1. TGA results for PLA composites.

Sample	$T_{-2wt\%}$(˚C)	T_{max}(˚C)	Char residue at 700˚C (wt%)
PLA1	307	362	0.6
PLA2	283	352	1.4
PLA3	262	343	2.6
PLA4	252	337	3.3
PLA5	237	330	4.9

RTIR is employed to evaluate chemical structure changes during thermal oxidative degradation. The spectra of PLA1 and PLA5 at different temperatures are described in Fig. 3. The peaks at 3002 and 2943 cm^{-1} corresponds to $–CH_3$ and –CH– stretching vibration. The 1762 cm^{-1} peak is assigned to C=O stretching vibration. The peaks at 1460 and 1380 cm^{-1} are attributed to –CH– deformation vibration. The 1186 and 1089 cm^{-1} peaks are stretching vibration of C-O-C [22]. As presented by Fig. 3 (a), the relative intensity of PLA1 peaks does not show obvious change below 300˚C. Then it is weakened at 330˚C. The characteristic peaks almost disappear above 360˚C. It is caused by the chain broken of PLA matrix. Thus, the main thermal oxidative degradation of neat PLA appears at 330~360˚C region. The thermal oxidative degradation curves of PLA5 are shown by Fig. 3 (b). At 330˚C, the relative intensity of $–CH_3$, –CH– stretching vibration, –CH– deformation vibration decrease apparently. At 360˚C, all of ester bonds pyrolyze according to the decrease of C=O peaks. Meanwhile, the stretching vibration of C-O-C nearly disappears. Actually, it is noted that all the absorption peaks nearly disappear when the temperature rises up to 360˚C, indicating that the main degradation process appears at this stage. This is consistent with TGA results (As discussed in Fig. 2 (b)). The representative degradation curves of PLA1 and PLA5 at different temperatures are illustrated in Fig. 3 (c). It could be seen that the biggest difference between PLA1 and

PLA5 appears at 330˚C. The characteristic intensity of PLA5 peaks is weaker than that of PLA1. It indicates that the addition of L. make the time of thermal oxidative degradation for PLA advance. These results are agreement with TGA analyses.

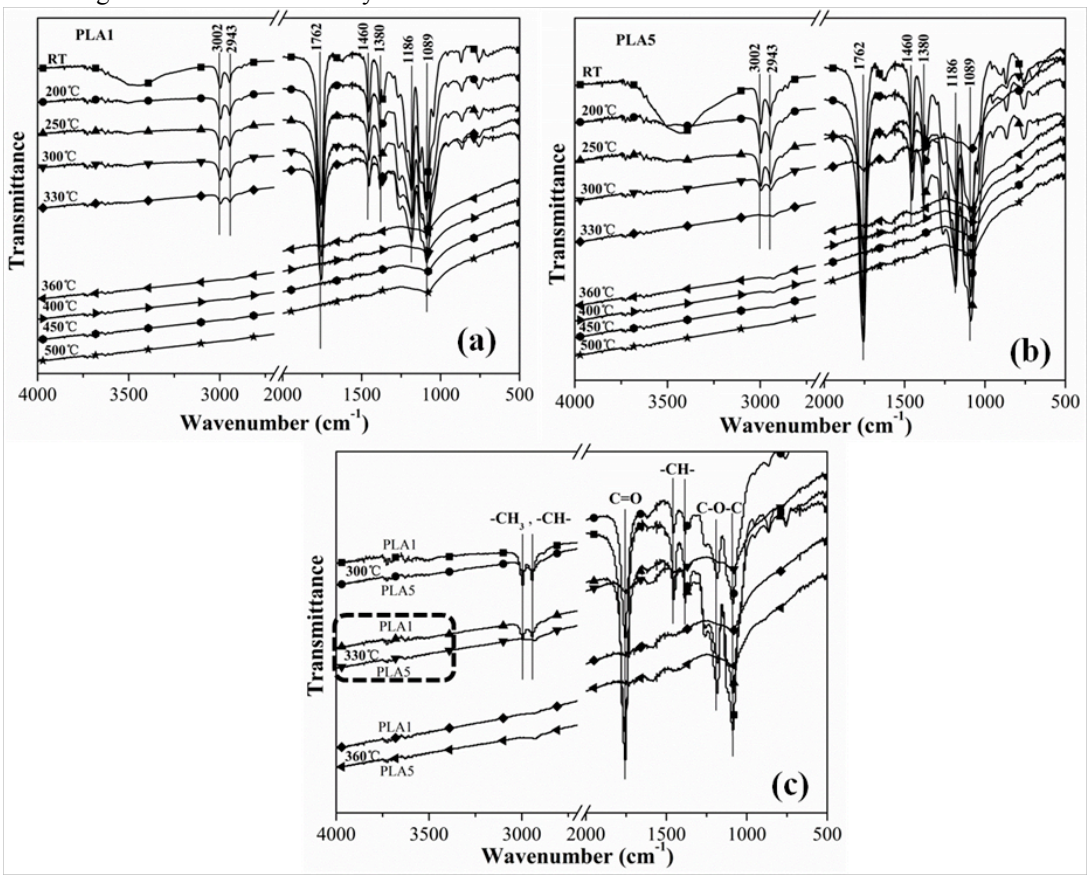

Fig. 3. (a) RTIR spectra of PLA1; (b) RTIR spectra of PLA5; (c) The representative RTIR curves of PLA1 and PLA5.

Combustible Property of PLA Composites

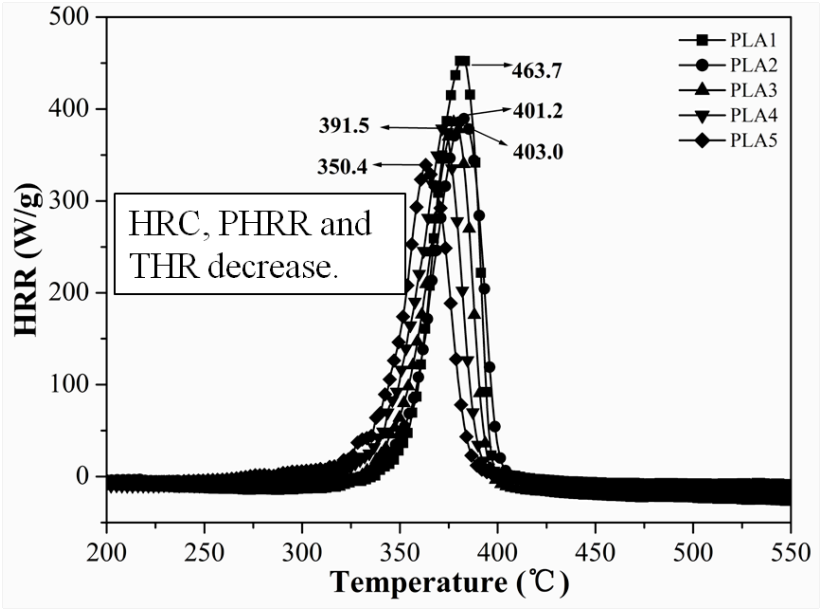

Fig. 4. HRR curves of PLA composites.

Figure 4 is the heat release rate (HRR) curves of PLA composites. The combustion data: High peak of heat release rate (PHRR) and the corresponding temperature (T_{max}), heat release capacity (HRC) and total heat release (THR) are presented in Table 2. HRC is a relatively good predictor of the heat release rate in flaming combustion and the propensity for ignition. The low value of HRC is indication of low flammability and low full scale fire hazard. Pure PLA is a flammable polymeric which has a high HRC, PHRR and THR. A significant reduction of these data for PLA composites is observed with the addition of L.. When the amount of L. is increased, HRC, PHRR and THR are decreased except for PLA3. PHRR value decreases from 463.7 W/g for pure PLA to 350.4 W/g for PLA5 with a reduction of 24.4%. HRC and THR value for PLA5 has a remarkable reduction of 22.8% and 6.3% in comparison with pure PLA, respectively. The summary results show that the presence of L. could reduce the fire risk of the PLA composites. It might be L. catalysis could enhance the carbonization of PLA composites in the thermal decomposition process and reduce the mass loss rate. The thermal decomposition products of L. may cover the residue of matrix and capture free radicals to obstruct or cut off the mass transfer path [23,24]. T_{max} corresponding to PHRR has a little change.

Table 2. MCC results for PLA composites.

Sample	HRC(J/g·˚C)	PHRR(w/g)	THR(kJ/g)	T_{max} (˚C)
PLA1	456	463.7	12.7	382
PLA2	396	401.2	12.5	382
PLA3	400	403.0	11.5	378
PLA4	390	391.5	12.0	373
PLA5	352	350.4	11.9	363

The Volatilized Products of PLA1 and PLA5

TGA-IR is performed to analyze the volatilized products after the sample pyrolysis, which is contributed to understand the thermal degradation mechanism. Figure 5 (a) shows the thermal degradation of PLA1 and PLA5 under N_2 atmosphere. Although $T_{-2\ wt\%}$ and T_{max} shift to the low regions, the char residue at 700˚C is changed from 0.9 wt% for PLA1 to 5.7 wt% for PLA5. The thermal stability of PLA at the high temperature is improved by the addition of L. It is agreement with Fig. 2 (b) analyses. The change of the total volatilized products with time is shown in Fig. 5 (b). The volatilized product release of PLA1 begins at 12.2 min. It increases until reaches the maximum at 15.0 min, then decreases. After 18.4 min, it cannot be observed in the curve. While that of PLA5 appears at 11.8 min, and the time of maximum peak is 13.7 min. It disappears at 17.1 min. It reveals that the time of volatilized product release is shifted to a small time region after adding L.. Therefore, L. could accelerate the pyrolysis of PLA matrix, as Fig. 3 discussion. The amount of total volatilized products is decreased with L. additives. It suggests that L. might prohibit PLA matrix combustion and reduce the generation of gases. The combustible gases in these volatilized products can accelerate the spread of heat and mass. Thus, L. could improve the fire security of PLA. The relationship between the intensity of characteristic peaks and time is shown in Fig. 5 (c) and (d). Some volatilized products, such as hydrocarbon and CO_2 are identified easily by their characteristic absorbance: The peak at about 2771 cm^{-1} is attributed to hydrocarbon. CO_2 peak corresponds to 2338 cm^{-1}. The change trends of hydrocarbon and CO_2 with time are similar to Fig. 5 (b), which indicates that L. could accelerate the generation of volatilized products in PLA matrix. Hydrocarbon is easy to burn, increasing the fire risk of PLA substrate. Figure 5 (c) exhibits that the hydrocarbon content is reduced apparently when L. is added. Therefore, L. performs good effect in improving the fire security of PLA, associated with Fig. 5 (b) discussions. Figure 5 (d) presents that CO_2 yield is increased significantly. CO_2 is an incombustible gas, which dilutes the fuel in gaseous phase so that the lower ignition limit of the gas mixture might be not reached. In summary, the incorporation of L. has a positive effect in PLA matrix.

DMA Measurement

The storage modulus variation of PLA composites is presented in Fig. 6. It indicates that the storage modulus is increased with the amount of L. increase. Therefore, L. additive has the reinforcing effect for PLA, which enhance storage modulus.

CONCLUSIONS

Nickel-containing ligand (L.) decorated with molybdenum and 1h-pyrazole template was prepared by the hydrothermal technique. Then it was added in PLA matrix. The effect of L. on the thermal stability,

combustible property and mechanical property of PLA matrix was investigated. L. could accelerate the thermal decomposition or degradation of PLA matrix at the low temperature region. However, it increased the thermal stability of matrix at the high temperature region. In addition, L. additive could improve the plasticity, fire security and storage modulus of PLA. Therefore, the results revealed that L. had the positive effect in PLA matrix.

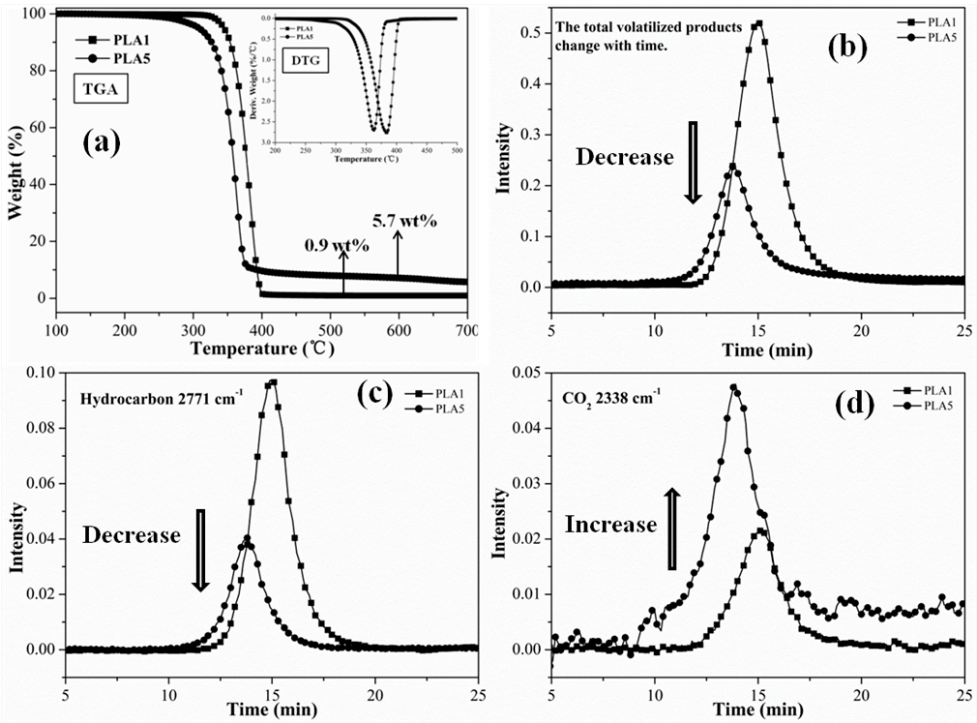

Fig. 5. (a) The TGA curves of PLA1 and PLA5 under N_2 atmosphere; (b) The change of the total volatilized products with time; (c) The change of hydrocarbon with time; (d) The change of CO_2 with time.

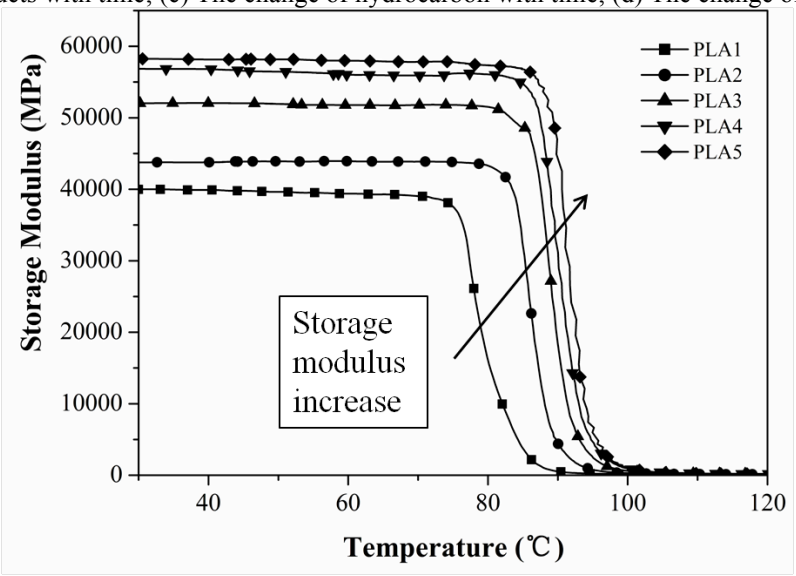

Fig. 6. DMA curves of PLA composites.

ACKNOWLEDGMENTS

This work was financially supported by joint funding by the National Basic Research Program of China (973 Program) (2012CB719701), National Natural Science Foundation of China (No.51036007) and China Postdoctoral Science Foundation (2012M521246).

REFERENCES

[1] Fortunati, E., Armentano, I., Zhou, Q., Lannoni, A., Saino, E., Visai, L., Berglund, L. A. and Kenny, J. M., (2012) Multifunctional bionanocomposite films of poly(lactic acid), cellulose nanocrystals and silver nanoparticles, Carbohydrate Polymers 87: 1596-1605, http://dx.doi.org/10.1016/j.carbpol.2011.09.066

[2] Liu, H., Chen, N., Fujinami, S., Louzguine-Luzgin, D., Nakajima, K. and Nishi, T., (2012) Quantitative nanomechanical investigation on deformation of poly(lactic acid), Macromolecules 45: 8770-8779, http://dx.doi.org/10.1021/ma301961h

[3] Porras, A., and Maranon, A., (2012) Development and characterization of a laminate composite material from polylactic acid (PLA) and woven bamboo fabric, Composites Part B-Engineering 43: 2782-2788, http://dx.doi.org/10.1016/j.compositesb.2012.04.039

[4] Wang, D. Y., Gohs, U., Kang, N. J., Leuteritz, A., Boldt, R., Wagenknecht, U. and Heinrich, G., (2012) Method for simultaneousiy improving the thermal stability and mechanical properties of poly(lactic acid): Effect of high-energy electrons on the morphological, mechanical, and thermal properties of PLA/MMT nanocomposites, Langmuir 28: 12601-12608, http://dx.doi.org/10.1021/la3025099

[5] Chang, S. K., Zeng, C., Yuan, W. Z. and Ren, J., (2012) Preparation and characterization of double-layered microencapsulated red phosphorus and its flame retardance in poly(lactic acid), Journal of Applied Polymer Science 125: 3014-3022, http://dx.doi.org/10.1002/app.36449

[6] Gonzalez, A., Dasari A., Herrero, B., Plancher, E., Santaren, J., Esteban, A. and Lim, S. H., (2012) Fire retardancy behavior of PLA based nanocomposites, Polymer Degradation and Stability 97: 248-256, http://dx.doi.org/10.1016/j.polymdegradstab.2011.12.021

[7] Wei, L. L., Wang, D. Y., Chen, H. B., Chen, L., Wang, X. L. and Wang, Y. Z., (2011) Effect of a phosphorus-containing flame retardant on the thermal properties and ease of ignition of poly(lactic acid), Polymer Degradation and Stability 96: 1557-1561, http://dx.doi.org/10.1016/j.polymdegradstab.2011.05.018

[8] Li, S. M., Yuan, H., Yu, T., Yuan, W. Z. and Ren, J., (2009) Flame-retardancy and anti-dripping effects of intumescent flame retardant incorporating montmorillonite on poly(lactic acid), Polymers for Advanced Technologies 20: 1114-1120, http://dx.doi.org/10.1002/pat.1372

[9] Liu, X. Q., Wang, D. Y., Wang, X. L., Chen, L. and Wang, Y. Z., (2011) Synthesis of organo-modified alpha-zirconium phosphate and its effect on the flame retardancy of IFR poly(lactic acid) systems, Polymer Degradation and Stability 96: 771-777, http://dx.doi.org/10.1016/j.polymdegradstab.2011.02.022

[10] Wang, D. Y., Leuteritz, A., Wang, Y. Z., Wagenknecht, U. and Heinrich, G., (2010) Preparation and burning behaviors of flame retarding biodegradable poly (lactic acid) nanocomposite based on zinc aluminum layered double hydroxide, Polymer Degradation and Stability 95: 2474-2480, http://dx.doi.org/10.1016/j.polymdegradstab.2010.08.007

[11] Yanagisawa, T., Kiuchi, Y., and Iji, M., (2009) Enhanced flame retardancy of polylactic acid with aluminum tri-hydroxide and phenolic resins, Kobunshi Ronbunshu 66: 49-54, http://dx.doi.org/10.1295/koron.66.49

[12] Lin, N., Huang, J., Chang, P. R., Feng, J. W. and Yu, J. H., (2011) Surface acetylation of cellulose nanocrystal and its reinforcing function in poly(lactic acid), Carbohydrate Polymers 83: 1834-1842, http://dx.doi.org/10.1016/j.carbpol.2010.10.047

[13] Marais, A., Kochumalayil, J. J., Nilsson, C., Fogelstrom, L. and Gamstedt, E. K., (2012) Toward an alternative compatibilizer for PLA/cellulose composites: Grafting of xyloglucan with PLA, Carbohydrate Polymers 89: 1038-1043, http://dx.doi.org/10.1016/j.carbpol.2012.03.051

[14] Shi, Q. F., Zhou, C. J., Yue, Y. Y., Guo, W. H., Wu, Y. Q. and Wu, Q. L., (2012) Mechanical properties and in vitro degradation of electrospun bio-nanocomposite mats from PLA and cellulose nanocrystals, Carbohydrate Polymers 90: 301-308, http://dx.doi.org/10.1016/j.carbpol.2012.05.042

[15] Guo, H. X., Wang, Q. H., Chen, C., Liang, M. and Chen, L., (2008) A novel one-dimensional reduced Molybdenum(V) decorated with nickel coordination cations:

$Ni[Mo_6O_{12}(OH)_3(PO_4)(HPO_4)_3]_2[Ni(H_2O)_2][Ni(H_2O)(bipy)_2]_4$ center dot $5H_2O$, Chinese Journal of Chemistry 26: 640-644, http://dx.doi.org/10.1002/cjoc.200890121

[16] Liu, L., Li, J., Sun, Z. G., Dong, D. P., Zhang, N., Lu, X., Wang, W. N. and Tong, F., (2010) Hydrothermal synthesis, crystal structure and characterizations of four new metal phosphonates with layered structure, Zeitschrift fur Anorganische und Allgemeine Chemie 636: 247-252, http://dx.doi.org/10.1002/zaac.200900285

[17] Sun, Y. H., Xu, J. Q., Ye, L., Cui, X. B., Li, Y., Yu, H. H., Li, G. H., Yang, G. D. and Chen, Y., (2005) Hydrothermal synthesis and crystal structural characterization of two new modified polyoxometalates constructed of positive and negative metal-oxo cluster ions, Journal of Molecular Structure 740: 193-201, http://dx.doi.org/10.1016/j.molstruc.2005.01.028

[18] Thomas, J., and Ramanan, A., (2011) Phosphomolybdate cluster based solids mediated by transition metal complexes, Inorganica Chimica Acta 372: 243-249, http://dx.doi.org/10.1016/j.ica.2011.02.028

[19] Araujo, A. B. A., Lemos, A. F., and Ferreira, J. M. F., (2009) Rheological, microstructural, and in vitro characterization of hybrid chitosan-polylactic acid/hydroxyapatite composites, Journal of Biomedical Materials Research Part A 88A: 916-922, http://dx.doi.org/10.1002/jbm.a.31949

[20] Liu, Y., Li Y. X., Zhang, S. W., Ji, H. M., Cao, R. G. and Liu, S. X., (2009) Organic-inorganic hybrid based on the molybdenum tellurite, Journal of Molecular Structure 921: 114-117, http://dx.doi.org/10.1016/j.molstruc.2008.12.058

[21] Han, L. J., Han, C. Y., Zhang, H. L., Chen, S. and Dong, L. S., (2012) Morphology and properties of biodegradable and biosourced polylactide blends with poly(3-hydroxybutyrate-co-4-hydroxybutyrate), Polymer Composites 33: 850-859, http://dx.doi.org/10.1002/pc.22213

[22] Zhan, J., Song, L., Nie, S. B. and Hu, Y. A., (2009) Combustion properties and thermal degradation behavior of polylactide with an effective intumescent flame retardant, Polymer Degradation and Stability 94: 291-296, http://dx.doi.org/10.1016/j.polymdegradstab.2008.12.015

[23] Le Bras M, Bourbigot, S., and Christelle, D., (1996) New Intumescent formulations of fire-retardant polypropylene-discussion of the free radical mechanism of the formation of carbonaceous protective material during the thermo-oxidative treatment of the additives, Fire and Materials 20 (4): 191–203, http://dx.doi.org/10.1002/(SICI)1099-1018(199607)20:4<191::AID-FAM577>3.0.CO;2-S

[24] Nie, S. B., Hu, Y., Song, L., He, S. Q. and Yang, D. D., (2008) Study on a novel and efficient flame retardant synergist-nanoporous nickel phosphates VSB-1 with intumescent flame retardants in polypropylene, Polymers for Advanced Technologies 19: 489-495, http://dx.doi.org/10.1002/pat.1088